Journal of Quantitative Spectroscopy & Radiative Transfer 252 (2020) 107063

Contents lists available at ScienceDirect

Journal of Quantitative Spectroscopy & Radiative Transfer

journal homepage: www.elsevier.com/locate/jqsrt

Complex refractive indices measurements of polymers in infrared bands

Xiaoning Zhang[a], Jun Qiu[a,c,d,*], Junming Zhao[a,c], Xingcan Li[a,e], Linhua Liu[a,b]

[a] School of Energy Science and Engineering, Harbin Institute of Technology, 92, West Dazhi Street, Harbin 150001, China
[b] School of Energy and Power Engineering, Shandong University, Qingdao 266237, China
[c] Key Laboratory of Aerospace Thermophysics, Ministry of Industry and Information Technology, Harbin Institute of Technology, Harbin 150001, China
[d] State Key Lab of Digital Manufacturing Equipment and Technology, Huazhong University of Science and Technology, Wuhan, Hubei 430074, China
[e] College of Energy and Power Engineering, Northeast Electric Power University, Jilin, 132012, China

ARTICLE INFO

Article history:
Received 16 February 2020
Revised 31 March 2020
Accepted 30 April 2020
Available online 26 May 2020

Keywords:
Spectroscopic ellipsometry
Ray tracing method
Complex refractive index
Polymer
Kramers-Kronig relations
Absorption peak

ABSTRACT

Polymers are widely used in many fields such as radiative cooling, infrared stealth, optical fibers and solar cells. In this work, the complex refractive indices of seven polymers such as polydimethylsiloxane (PDMS), polymethyl methacrylate (PMMA), polycarbonate (PC), polystyrene (PS), polyethylene terephthalate (PET), polyvinyl chloride (PVC), and polyetherimide (PEI) are measured by spectroscopic ellipsometry (SE) combined with the ray tracing method (RTM) from near-infrared to mid-infrared bands (2–20 μm). The measured results of PDMS have been proved to be accurate by comparing them with previous data in the literature. The obtained refractive indices of polymers in this paper have been compared with the results calculated by the Kramers-Kronig relations. Finally, we analyze the reasons of absorption peaks of these materials in infrared bands by the vibration of chemical bonds in molecules.

1. Introduction

In recent years, many researches have been devoted to the polymers for their good application prospects in radiative cooling, infrared stealth and solar cells [1,2]. Polymers have been widely used as matrix of coatings for radiative cooling because of their lower qualities and good optical characteristics. We should know the radiative properties of polymers as accurately as possible in order to design the radiative cooling systems properly. But the precise complex refractive indices of polymers are still very rare now which maybe creating some problems in the research. Huang et al. [3] added TiO_2 and carbon black to polymethyl methacrylate (PMMA) and obtained the radiation characteristics of double-layer coating in 0.3–26 μm and the radiative cooling power by numerical calculation. Due to the lack of complex refractive index of PMMA, it is assumed in the calculation that the extinction coefficient of PMMA is 0. In fact, the formula of PMMA contains chemical bonds such as C–H and C–C [4], and there should be multiple absorption peaks in infrared bands. Hence the assumption about the extinction coefficient of PMMA in the literature may not be appropriate. Yang et al. [5] embedded randomly distributed SiO_2 microspheres into polymethylpentene (TPX) film, and calculated the complex refractive index and radiation characteristic of composite structure by using the effective medium theory. The absorption peaks of TPX in infrared bands are attributed to the Fröhlich resonance in Ref. [5]. Actually the formula of TPX contains several C–H and some absorption peaks of TPX will be generated in infrared bands as a result of the vibration of chemical bonds. So the analysis of strong absorption in infrared bands of the composite structure in Ref. [5] may not be appropriate. The Ref. [3] and Ref. [5] show that only after obtaining the accurate complex refractive index of the polymer can we analyze and solve the problem of radiation characteristics better.

The spectroscopic ellipsometry (SE) is generally considered to be the most accurate method for measuring complex refractive indices of materials with strong absorption. The complex refractive indices of some polymers have been measured by SE because of its high precision and non-destructive properties [6–8]. However, SE has a limitation in measuring the highly transparent bands of single-layer substrate [9]. So that we introduce the ray tracing method (RTM) to make up for this deficiency. The RTM is a commonly used method to calculate the complex refractive index of material with weak absorption [10,11]. The SE and RTM are complementary so that we combine them to measure the complex refractive indices of polymers in the wavelength range of 2–20 μm. This paper reports the measured complex refractive in-

* Corresponding author.
E-mail address: qiujun@hit.edu.cn (J. Qiu).

https://doi.org/10.1016/j.jqsrt.2020.107063
0022-4073/

dices of polydimethylsiloxane (PDMS) with different ratios of composition, PMMA, polycarbonate (PC), polystyrene (PS), polyethylene terephthalate (PET), polyvinyl chloride (PVC) and polyetherimide (PEI) in the 2–20 μm range by SE combined with the RTM, and discusses the reasons why these polymers have absorption peaks in infrared bands.

2. Methods and experimental setup

2.1. Spectroscopic ellipsometry combined with the ray tracing method

The SE can obtain precise ellipsometric parameters by measuring the beam intensity attenuation and phase change caused by reflection. The ellipsometric parameters ψ and Δ are related to the reflection coefficients R_p and R_s. p and s represent the horizontally and vertically polarized component in the direction of mirror reflection of sample surface, respectively [12].

$$\tilde{\rho}=\frac{R_p}{R_s}=\tan(\psi)e^{i\Delta}=\left(\frac{E_{rp}}{E_{ip}}\right)/\left(\frac{E_{rs}}{E_{is}}\right) \tag{1}$$

$\tilde{\rho}$contains both intensity and phase information of reflected light in ellipsometric measurements. $\tan(\psi)$ and Δ represent amplitude and phase difference of $\tilde{\rho}$, respectively. The complex refractive index $n + ik$ is obtained by inversion after measuring the ellipsometric parameters. Its real part is refractive index n and the imaginary part is extinction coefficient k. The true value in inversion process is the measured ψ and Δ. The model should be set in the WVASE32 software based on structure and optical property of the sample. When the deviation between the ellipsometric parameters fitted by theoretical model and the measured is within a certain range, the complex refractive index of theoretical model is considered to be the result we need. The deviation is expressed as following objective function [12]:

$$MSE=\sqrt{\frac{1}{2M-N}\sum_{j=1}^{M}\left[\left(\frac{\psi_j^{\mathrm{mod}}-\psi_j^{\exp}}{\sigma_{\psi,j}^{\exp}}\right)^2+\left(\frac{\Delta_j^{\mathrm{mod}}-\Delta_j^{\exp}}{\sigma_{\Delta,j}^{\exp}}\right)^2\right]} \tag{2}$$

Where M and N are the number of measured ψ-Δ pairs and the parameters to be fitted in the model, respectively. σ is the standard deviation of experimental measurement data points. We hold that the results obtained are credible when the value of *MSE* is less than or equal to 1. This paper only studies the case of measuring substrates.

The measured polymers are single-layer and the surface roughness parameters Ra of samples are less than 0.006 μm. Hence the effect of surface roughness on the results can be ignored. We can set an air-polymer model in the WVASE32 software and use the measured ellipsometric parameters of polymers as input values. The complex refractive indices of polymers are selected as the parameters to be fitted in the WVASE32 software and the results will be obtained after the end of the fitting process. Due to the superiority of the measurement principle, SE is currently considered to be the most accurate method for measuring complex refractive indices of opaque substrates [13].

For opaque substrates, the above method (SE) is applicable. But it's not suitable to measure the complex refractive indices of highly transparent substrates by SE. Fig. 1 shows the normal transmittance t of PMMA (Mitsubishi) in the spectral range of 2–20 μm. From Fig. 1 we can know that the normal transmittance of PMMA are higher near 2 μm and are almost equal to 0 at other bands. This paper uses the value of normal transmittance to determine the transparency of the sample. When the normal transmittance of single-layer sample is less than or almost equal to 0.01, we hold that the sample is opaque and the results obtained by SE is credible. If the normal transmittance of sample is much larger than 0.01,

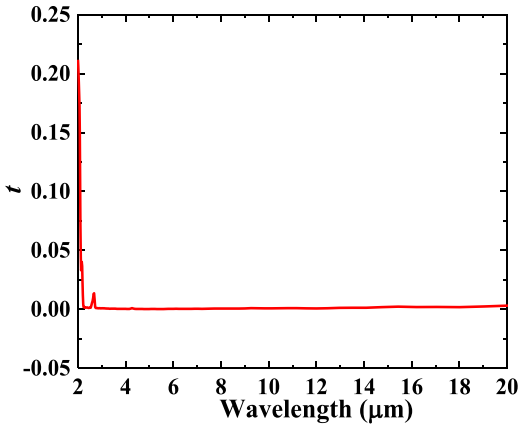

Fig. 1. The normal transmittance of PMMA in 2–20 μm.

an accurate complex refractive index may not be obtained directly using SE.

The method of sub-band measurement is used to obtain the complex refractive index of PMMA in the spectral range of 2–20 μm. For the opaque bands of PMMA (2.21–20 μm), the complex refractive index (n and k) can be obtained by SE. The normal transmittance of PMMA in 2–2.21 μm is much great than 0.01. In this case, the precise refractive index n can be obtained but not the extinction coefficient k [9]. The reason is that the PMMA is thick enough, and there is no "back-reflection" during the measurement. The "back-reflection" is that the detector of the ellipsometer will receive the reflected light from the top and back surfaces at the same time, thus creating a depolarization effect. We can eliminate the effect of "back-reflection" by increasing the thickness or polishing the back of sample [9]. After we obtain the normal transmittance t and refractive index n of highly transparent substrate, the RTM can be introduced to calculate the extinction coefficient k of PMMA in 2–2.21 μm. The equations of RTM are expressed as follows [14]:

$$\rho=\frac{(n-n_0)^2+(k-k_0)^2}{(n+n_0)^2+(k+k_0)^2} \tag{3}$$

$$\tau=1-\rho \tag{4}$$

$$\varepsilon=\exp\left(-\frac{4\pi kL}{\lambda}\right) \tag{5}$$

$$t=\frac{\tau^2\varepsilon}{1-\rho^2\varepsilon^2} \tag{6}$$

The n_0+ik_0, $n+ik$, ρ, τ, ε and L represent the complex refractive index of air and sample, the reflectance and transmittance of interface, internal transmittance and the thickness of sample, respectively. The complex refractive indices of all other polymers in this paper have been obtained by SE combined with the RTM. When the thickness of measured substrate is very small (only a few microns), the method used in this paper will not work. We can use the way proposed by Zhang et al. [15] to measure the complex refractive index of the sample at this time.

2.2. Experimental procedure and sample preparation

The sizes, thicknesses, manufactures and surface roughness parameters Ra of PDMS, PMMA, PC, PS, PET, PVC and PEI are given in Table 1 [9]. The measuring instrument is the IR-VASE spectroscopic ellipsometer (J.A. Woollam Company) which measures from

Table 1
Size, Thickness, Manufacturer and Surface Roughness Parameter Ra of the Samples [9].

Sample	Shape	Surface Size (mm)	Thickness (mm)	Manufacturer	Surface Roughness Parameter Ra (nm)
PDMS	cylinder	diameter=35	10.5 (5:1), 11.2 (10:1), 10.1 (15:1), 10 (20:1),	Dow Corning, America	1.35
PMMA	cuboid	20 × 20	10	Tomson, China Mitsubishi, Japan	0.866
PC	cuboid	20 × 20	10	Dedicated Plastic, China	1.41
PS	cuboid	20 × 20	7.5	Shanghai Huineng Industry, China	0.922
PET	cuboid	20 × 20	4	Chenghang Plastic Technology, China	0.647
PVC	cuboid	25 × 25	5	Jubang plastic material, China	1.32
PEI	cylinder	diameter=25	4.6	Winning engineering plastic, China	3.87

1.5 to 40 μm. The spectral resolution was set to 16 cm^{-1} in order to obtain peaks of complex refractive indices of polymers accurately. The incident angles of ellipsometer are 65°, 70°, and 75° The measured PDMS is classified into x = 5:1, x = 10:1, x = 15:1 and x = 20:1 according to the mass ratio of main agent to curing agent, and x represents mass (main agent): mass (curing agent). The effect of the mass ratio x on the complex refractive index of PDMS in 2–20 μm is investigated in this work. The measured polymers in this paper are all optical isotropic and all measurements were made at room temperature and pressure.

2.3. Experimental uncertainty

The complex refractive index (n and k) of each sample is measured 6 times. For opaque bands of polymer, the average of the results and uncertainty can be expressed as [16]

$$\bar{\xi}_{\exp} = \frac{1}{M}\sum_{i=1}^{M}\xi_{\exp,i} \tag{7}$$

$$\Delta\bar{\xi}_{\exp} = \sqrt{\frac{1}{M}\sum_{i=1}^{M}\left(\xi_{\exp,i} - \bar{\xi}_{\exp}\right)^2} \tag{8}$$

Where $\xi_{\exp}$ and M = 6 represent the obtained complex refractive index and the number of measurements, respectively.

The average of complex refractive index (n and k) of highly transparent substrate is also obtained by Eq. (7) and the uncertainty of refractive index n is calculated by Eq. (8). The extinction coefficient k of highly transparent band of polymer is calculated by the thickness L, normal transmittance t and refractive index n of sample,

$$k_\lambda = f(t, n_\lambda, L) \tag{9}$$

The uncertainty of extinction coefficient k is calculated by the error propagation method [17].

$$(\Delta k_\lambda)^2 = \sum_i \left[\frac{\partial k_\lambda}{\partial x_i}\cdot\Delta x_i\right]^2 \approx \sum_i \left[\frac{k_\lambda(x_i+\delta x_i) - k_\lambda(x_i-\delta x_i)}{2\delta x_i}\cdot\Delta x_i\right]^2 \tag{10}$$

Where Δx_i represents the uncertainty of measured parameters t, L and n_λ. The uncertainty of thickness ΔL is 0.1 mm in this paper.

3. Results and discussion

3.1. The complex refractive indices of PDMS with different ratios of composition

The complex refractive index of PDMS has been studied experimentally in Refs. [18,19]. Schneider has obtained the refractive index of PDMS in 0.35–0.7 μm [18] and Querry measured the complex refractive index of PDMS in 2.5–56 μm [19]. The extinction coefficient of PDMS hasn't been measured in Ref. [18] and the composition of PDMS wasn't described in detail in Ref. [19]. Our group has been measured the complex refractive indices of these seven polymers in the 0.4–2 μm range previously [9]. The results in Ref. [9] show that the complex refractive indices of PDMS with different ratios of composition x (x = mass (main agent): mass (curing agent)) have slightly differences in 0.4–2 μm. We continue to study the effect of x on the complex refractive index of PDMS in 2–20 μm in this paper.

Taking PDMS as an example to verify the accuracy of SE combined with the RTM measuring the complex refractive indices of single-layer polymers. The complex refractive indices of PDMS with different ratios of composition in 2–20 μm are shown in Fig. 2 and compared with Querry's result [19]. Fig. 2 depicts that the complex refractive indices of PDMS with different ratios x of composition in 2–20 μm have similar trends as wavelength increases. The complex refractive index of PDMS measured in this paper is obvious different from the values of some wavelengths in Ref. [19] (such as 8 μm and 13 μm), which is mainly due to the differences in composition of the measured PDMS. The results indicated that x has little effect on the complex refractive index of PDMS in infrared bands and it maybe because the basic structure of PDMS has been fixed when x = 20:1 [9]. The curing agent will be randomly distributed in the sample and the composition of formula of curing agent is similar to main agent [20]. In addition, the mass fraction of curing agent in the total is relatively small (5%–20%). Hence the optical characteristics of PDMS will not be changed obviously as x alters between 5:1 and 20:1. But in order to ensure high accuracy in the calculation, it is necessary to measure the complex refractive indices of PDMS with different ratios of composition. Fig. 2 shows that SE combined with the RTM can obtain accurate results of the complex refractive indices of polymers.

3.2. The complex refractive index of PMMA

The research on the complex refractive index of PMMA is limited to visible to near-infrared bands at present [9,21,22] which limits the applications of PMMA. This work measured the complex

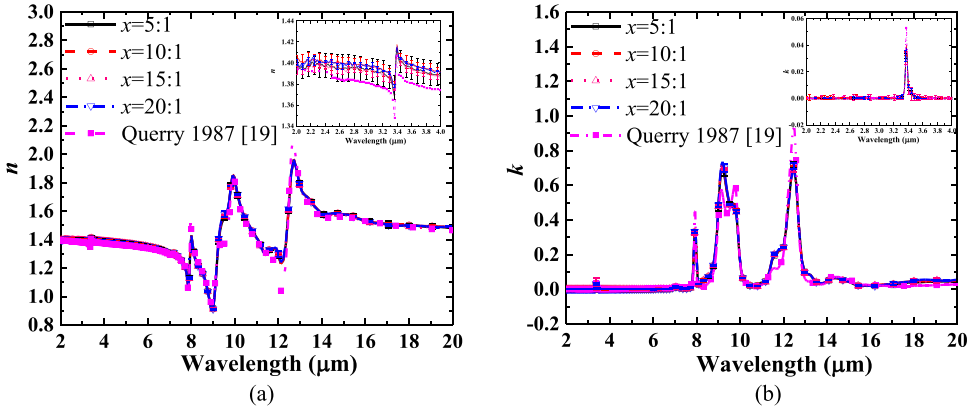

Fig. 2. The complex refractive indices of PDMS with different ratios *x* of composition in 2–20 μm and the published data. See **Data File 1** for underlying values. (a) refractive indices *n* (b) extinction coefficients *k*.

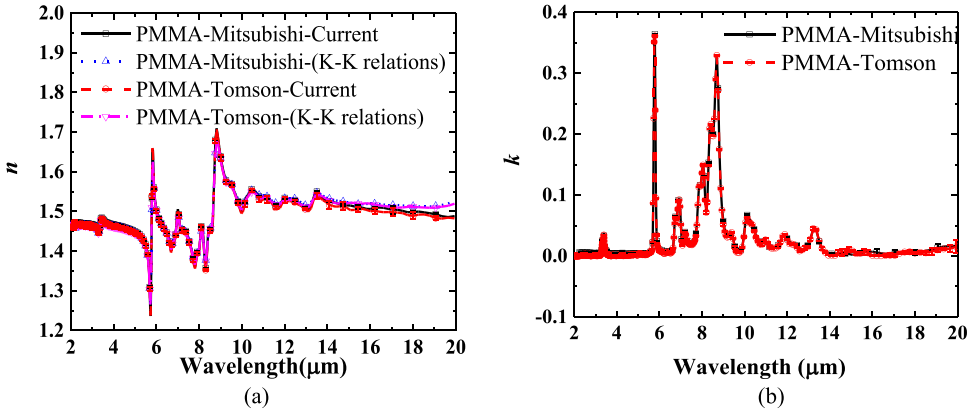

Fig. 3. The complex refractive indices of two PMMA samples in 2–20 μm. See **Data File 2** for underlying values. (a) refractive indices *n* (b) extinction coefficients *k*.

refractive index of PMMA in wider bands. The complex refractive indices of PMMA (Tomson) and PMMA (Mitsubishi) in the spectral range of 2–20 μm are presented in Fig. 3. The data measured by two PMMA samples have slightly differences which shows that the instability of industrial processes and injection parameters have some effects on the complex refractive index of PMMA in infrared bands. We can calculate the refractive index of PMMA according to the Kramers-Kronig relations [23]. The comparison between the calculated refractive indices by the Kramers-Kronig relations and the measured results is shown in Fig. 3(a). It is indicated that the refractive indices of the PMMA produced by two manufacturers almost coincide with the results obtained by the Kramers-Kronig relations. The part of the Kramers-Kronig relations can be expressed as follows [23]:

$$n(w) - 1 = \frac{2}{\pi} P \int_0^{\infty} \frac{w' k(w')}{w'^2 - w^2} dw' \tag{11}$$

Where *P* denotes the Cauchy principal value integral and the frequency is expressed as *w*. The Kramers-Kronig relations is an integral equation over the full spectrum. When using this method to calculate the refractive index over a limited wavelength range, the accuracy of Kramers-Kronig relations will closely related to the input spectral range. Hence the calculated and measured refractive index of PMMA are not exactly the same. The refractive index of PMMA decreases sharply in 5.12–5.74 μm, 5.81–6.68 μm and 8.82–9.33 μm, and it has an obvious increase in the spectral range of 5.74–5.81 μm and 6.82–7.01 μm. The refractive index of PMMA reaches a minimum of 1.24 at 5.74 μm and a maximum of 1.71 at 8.82 μm. The extinction coefficient of PMMA ups to a maximum of 0.36 at 5.79 μm and forms a sharp peak here. The extinction coefficient of PMMA has an apparently increase in 8.47–8.7 μm and owns a sharp decrease in 8.7–9.75 μm. The extinction coefficient of PMMA changes relatively slowly at other bands.

3.3. The complex refractive index of PC

The complex refractive index of PC in 2–20 μm is shown in Fig. 4. Only the refractive index of PC in visible to near-infrared bands was present previously [24]. The refractive index of PC has a sharp decrease in 5.69–6.2 μm, 6.68–7.95 μm and 8.64–9.19 μm, and increases obviously in 5.59–5.69 μm, 6.58–6.68 μm and 8.53–8.64 μm. The refractive index of PC reaches a minimum of 1.07 at 7.95 μm and has a maximum of 1.96 at 8.64 μm. The extinction coefficient of PC reaches 0.663 at 8.1 μm and forms a main absorption peak here. As shown in Fig. 4(a), we can know that the measured refractive index of PC in the region 2–20 μm is almost the same as the result calculated by the Kramers-Kronig relations. Fig. 5 shows the absorbance of a sample with a thickness of 2 μm in 1000–1800 cm^{-1} calculated by Eqs. (3)-(6) using the complex refractive index of PC measured in this paper, and the published data in Ref. [25]. The result exhibits that the variation trend of absorbance with wavelength calculated in this paper is consistent with that in the literature.

3.4. The complex refractive index of PS

The complex refractive index of PS in the wavelength range of 2–20 μm is shown in Fig. 6 and compared with the result in Ref. [26]. The blue line in Fig. 6(a) represents the calculated refractive index *n* from importing the measured extinction coefficient *k* of

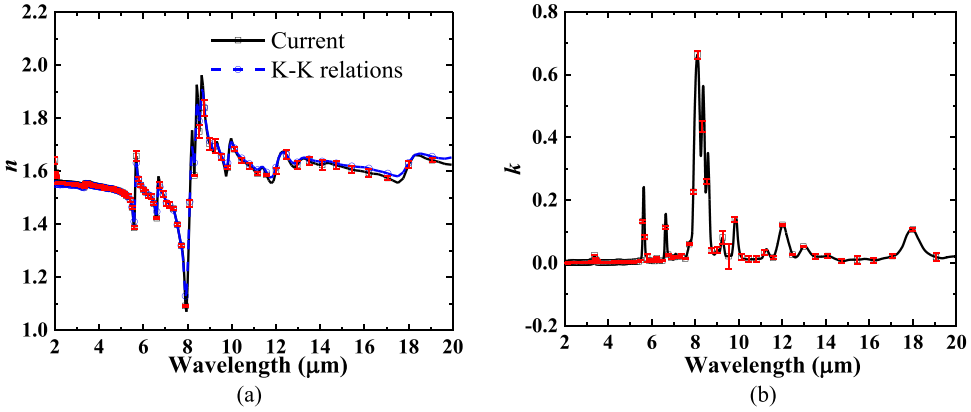

Fig. 4. The complex refractive index of PC in 2–20 μm. See **Data File 3** for underlying values. (a) refractive index n (b) extinction coefficient k.

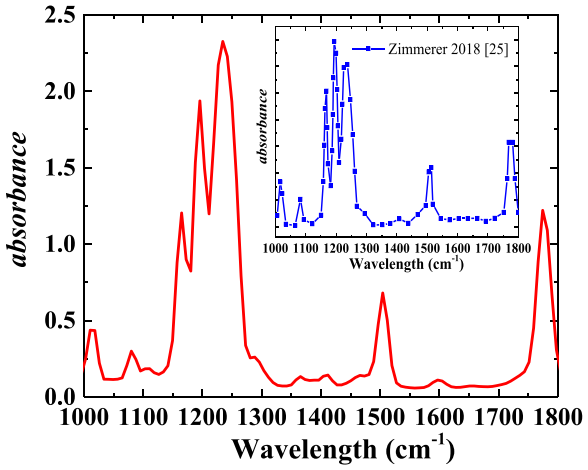

Fig. 5. The absorbance of PC with a thickness of 2 μm and the published data in the literature.

PS to Kramers-Kronig relations. As can be seen from Fig. 6(a), the measured refractive index of PS by SE combined with the RTM nearly coincides with the value obtained by the Kramers-Kronig relations. The relative difference between the refractive index n of PS that we measured and the results in Ref. [26] is no more than 10%. The refractive index of PS has a sharp decrease in 11.17–12.96 μm, 13.5–14.09 μm and 14.56–17.52 μm, and increases rapidly in 12.96–13.5 μm and 14.09–14.56 μm. The refractive index of PS reaches a minimum of 1.41 at 14.09 μm and gets to a maximum of 1.76 at 14.56 μm. The extinction coefficient of PS has a maximum of 0.322 at 14.24 μm and there is a sharp absorption peak here. The absorption peaks of PS also exist in 13.23 μm and 18.52 μm whose values are 0.105 and 0.064, respectively.

The data in Ref. [26] were obtained by importing the reflection-absorption spectrum (at 20°) of PS film deposited on copper surface to the RefFIT program to process. The green line in Fig. 6(a) shows the refractive index n was calculated by introducing the extinction coefficient k in Ref. [26] into the Kramers-Kronig relations. We can know from Fig. 6(a) that the calculated data is not consistent with the refractive index of PS in Ref. [26], which shows the complex refractive index of PS in Ref. [26] does not satisfy the Kramers-Kronig relations. The reason why the results measured in this paper are different from the data in Ref. [26] may be the measured injection molding process parameters of PS are different which affected the complex refractive index of the PS. Hence when the complex refractive index of material is very sensitive to the process parameters, we need to know the information of manufacturers or injection parameters of the sample clearly, and select the accurate values based on these messages.

3.5. The complex refractive index of PET

The measured complex refractive index of PET in 2–20 μm is shown in Fig. 7. At present, only the data ranges of the refractive index of PET (1.55–1.64) are available in Ref. [27]. The refractive index of PET decreases sharply in 5.84–6.82 μm, 8.1–8.82 μm, 9.19–9.75 μm and 13.94–19.35 μm, and has a significant increase in 5.74–5.84 μm, 7.72–8.1 μm, 8.82–9.19 μm and 13.5–13.94 μm. At the wavelengths of 8.1 μm and 7.72 μm, the refractive index of

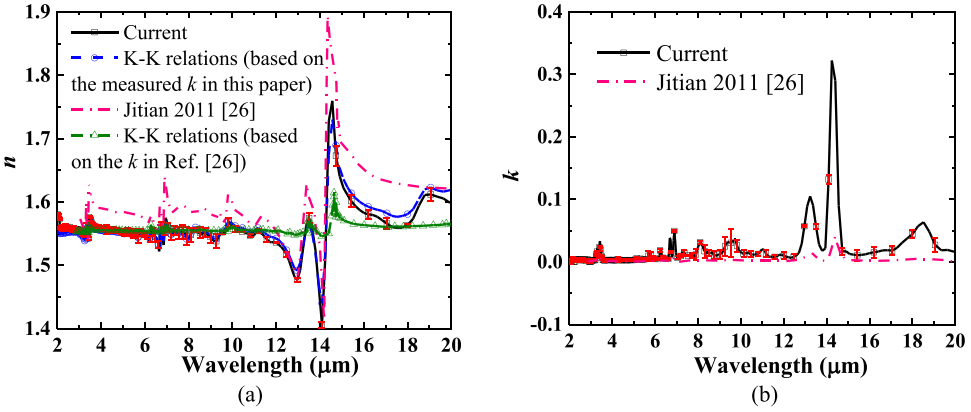

Fig. 6. The complex refractive index of PS in 2–20 μm. See **Data File 4** for underlying values. (a) refractive index n (b) extinction coefficient k.

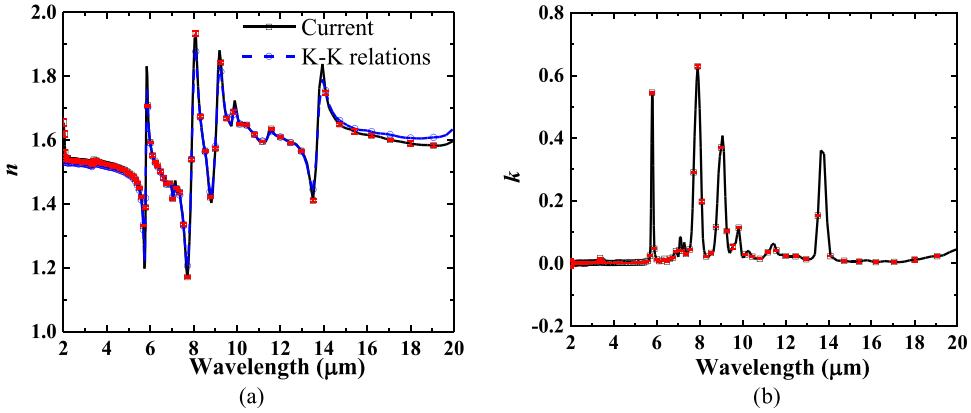

Fig. 7. The complex refractive index of PET in 2–20 μm. See **Data File 5** for underlying values. (a) refractive index *n* (b) extinction coefficient *k*.

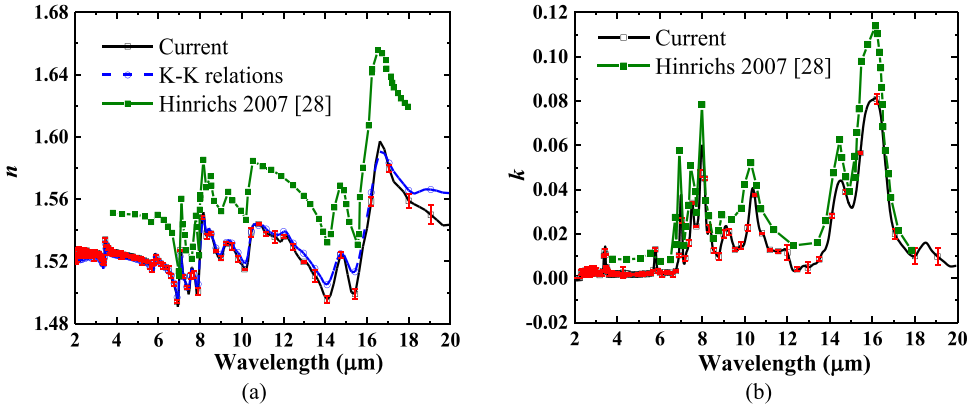

Fig. 8. The complex refractive index of PVC in 2–20 μm. See **Data File 6** for underlying values. refractive index *n* (b) extinction coefficient *k*.

PET reaches a maximum of 1.93 and a minimum of 1.17, respectively. The PET has absorption peaks at 5.79 μm, 7.9 μm, 9.06 μm and 13.65 μm with values of 0.545, 0.629, 0.408, and 0.361, respectively. From Fig. 7(a), we can know that the measured refractive index of PET agrees well with the calculated value by the Kramers-Kronig relations.

3.6. The complex refractive index of PVC

Fig. 8 presents the complex refractive index of PVC in the wavelength range of 2–20 μm and compared with reported data in Hinrichs [28]. The refractive index of PVC increases sharply in 7.86–8.15 μm and 15.43–16.6 μm, and has an apparent decrease in the spectral range of 8.15–8.31 μm and 16.6–19.64 μm. The refractive index of PVC reaches a maximum of 1.6 at 16.6 μm and gets to a minimum of 1.49 at 6.93 μm. The extinction coefficient of PVC attains a maximum of 0.08 at 16.2 μm. In Fig. 8(a), the relative difference between the measured refractive index of PVC and the calculated value is less than 2%.

The data in Ref. [28] (in the 4–18 μm range) were measured using bilayer model (a nanoscale single layer on a gold-coated glass substrate), and the instrument is the mid-infrared ellipsometer. The difference between the data measured in this paper and the results in Ref. [28] is mainly due to the different composition of the measured material.

3.7. The complex refractive index of PEI

Fig. 9 displays the complex refractive index of PEI in 2–20 μm. From Fig. 9(a), the measured refractive index of PEI is almost the same as the value calculated by the Kramer-Kronig relations. There is a significant oscillation in refractive index of PEI in 5–20 μm. At the wavelengths of 5.84 μm and 5.76 μm, the refractive index of PEI reaches a maximum of 1.82 and a minimum of 1.34, respectively. The extinction coefficient of PEI has a maximum of 0.453 at 5.79 μm and exists several absorption peaks in 5–20 μm.

3.8. Reasons for the formation of absorption peaks in infrared bands

The formulas of PDMS, PMMA, PS, PC, PVC, PET, and PEI are shown in Fig. 10 [4,20,29–33].

There are many obvious absorption peaks in 2–20 μm for these seven materials which are the results of deformation, bending and stretching of chemical bonds in the molecules. The absorption peak of PDMS near 9 μm owes to the stretching vibration of Si–O–Si. The absorption band of PDMS at 12.5 μm corresponds to the C–H asymmetrical rocking vibration in the -CH_3 and the asymmetrical stretching vibration of the Si-C [20]. The absorption peak of PMMA near 5.8 μm comes from the stretching vibration of C=O. In the region 6–10 μm, the absorption bands of PMMA are mainly attributed to the stretching vibration of C–O and C–C, and the deformation vibration of C–H in the -CH_3 [4]. The absorption peak of PS near 14.24 μm is related to the out of plane bending vibration of the C–H on the aromatic rings [26]. The absorption peak of PC near 8.1 μm is from the C–O–C stretching vibration [30]. The absorption peak of PVC near 16.2 μm comes from the stretching vibration of C–Cl [31]. The absorption bands of PET at 7.9 μm and 9.06 μm are assigned to C–O–C stretching vibration whereas bands near 13.65 μm are attributed to the bending vibration of C–H in -CH_3 [34]. The absorption bands of PEI in 7–9 μm correspond to the stretching vibration of C–N and the deformation vibration of aromatic rings [35].

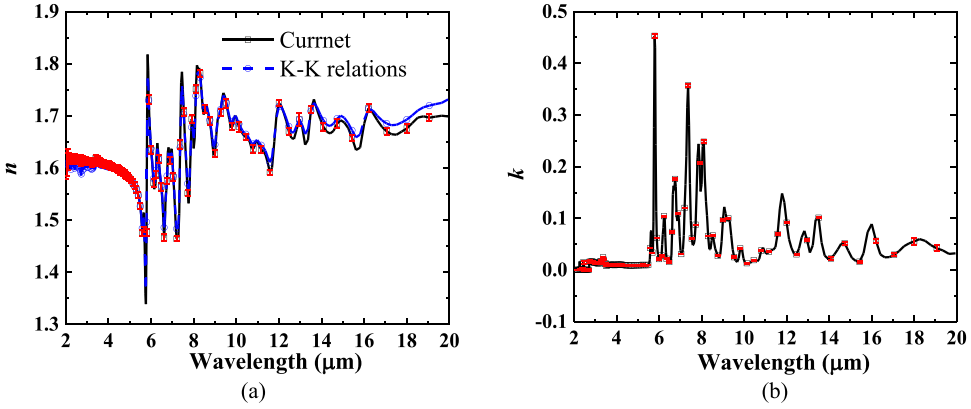

Fig. 9. The complex refractive index of PEI in 2–20 μm. See **Data File 7** for underlying values. (a) refractive index *n* (b) extinction coefficient *k*.

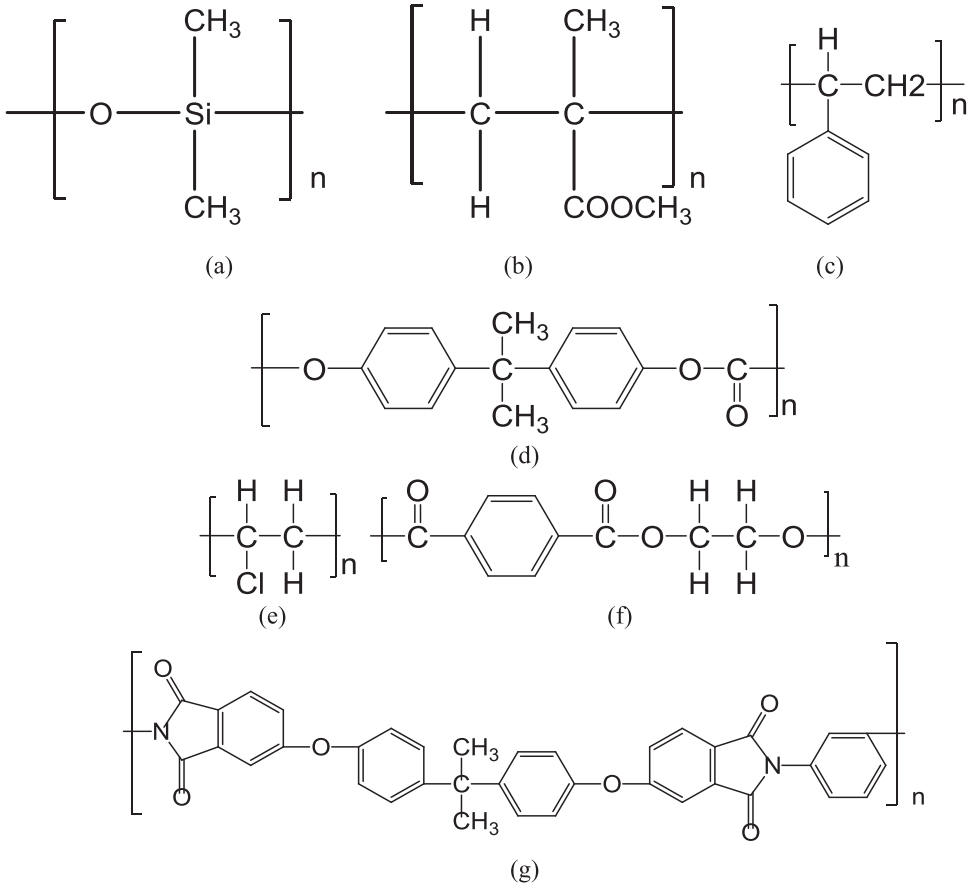

Fig. 10. Formulas: (a) PDMS [20] (b) PMMA [4] (c) PS [29] (d) PC [30] (e) PVC [31] (f) PET [32] (g) PEI [33].

We can find the specific application background of the material based on the absorption peaks of the polymers. When the material contains multiple C–H, C–N, C–C and C–O–C, the material will have many absorption peaks in the spectral range of 8–13 μm like PDMS, PMMA, PC, PET and PEI, and has good prospects for radiative cooling [3,5]. If the material contains C–Cl and aromatic rings, the material will have an absorption peak in 14–17 μm like PS and PVC, and the material may be added into the absorbing film of pyroelectric detector [36].

4. Conclusions

The complex refractive indices of seven polymers (PDMS, PMMA, PC, PS, PET, PVC and PEI) are measured by spectroscopic ellipsometry combined with the ray tracing method from near-infrared to mid-infrared bands (2–20 μm). The *MSE* fitted by the WVASE32 software is used to judge the credibility of the results obtained by spectroscopic ellipsometry when the absorption of materials is strong. When the *MSE* is less than or equal to 1 and the sample to be tested is almost opaque, it is considered that an accurate complex refractive index will be obtained. The spectroscopic ellipsometry can't directly obtain the extinction coefficients of highly transparent single-layer polymers, so that the ray tracing method is introduced to deal with this problem in this paper. The measured complex refractive indices of PDMS with different ratios of composition in the 2–20 μm range are almost identical to the data from the literature, which shows that the methods used in this work can obtain precise results. The obtained refractive in-

dices of polymers have been compared with the values calculated by the Kramers-Kronig relations. These seven materials have multiple absorption peaks in infrared bands and the reasons are related to the deformation, stretching and bending vibrations of chemical bonds. After obtaining the complex refractive indices of polymers, it is possible to explain the formation of absorption peaks in infrared bands and provide data support for the numerical simulation about polymers.

Declaration of Competing Interest

The authors declare that they have no known competing financial interests or personal relationships that could have appeared to influence the work reported in this paper.

CRediT authorship contribution statement

Xiaoning Zhang: Writing - original draft, Methodology. **Jun Qiu:** Supervision, Conceptualization, Methodology, Software. **Junming Zhao:** Data curation. **Xingcan Li:** Software. **Linhua Liu:** Methodology, Resources.

Acknowledgements

This work was supported by the National Natural Science Foundation of China (51336002, 51825601, 51621062).

Supplementary materials

Supplementary material associated with this article can be found, in the online version, at doi:10.1016/j.jqsrt.2020.107063.

References

[1] Schaub MP. The design of plastic optical systems. SPIE; 2009.
[2] Kou JL, Jurado Z, Chen Z, Fan SH, Minnich AJ. Daytime radiative cooling using near-black infrared emitters. ACS. Photonics 2017;4(3) 626–630.
[3] Huang ZF, Ruan XL. Nanoparticle embedded double-layer coating for daytime radiative cooling. Int J Heat Mass Transf 2017;104 890–896.
[4] Takashima K, Furukawa Y. Vibrational stark effect (VSE) on the infrared spectrum of a poly (methyl methacrylate) thin film. Vib Spectrosc 2015;78:54–9.
[5] Zhai Y, Ma Y, David SN, Zhao D, Lou R, Tan G, et al. Scalable-manufactured randomized glass-polymer hybrid metamaterial for daytime radiative cooling. Science 2017;355(6329) 1062–1066.
[6] Winfield JM, Donley CL, Kim JS. Anisotropic optical constants of electroluminescent conjugated polymer thin films determined by variable-angle spectroscopic ellipsometry. J App Phys 2007;102(6):063505.
[7] Karabiyik U, Mao M, Satija SK, Esker AR. Determination of thicknesses and refractive indices of polymer thin films by multiple incident media ellipsometry. Thin Solid Films 2014;565:72–8.
[8] Hilfiker JN, Stadermann M, Sun J. Determining thickness and refractive index from free-standing ultra-thin polymer films with spectroscopic ellipsometry. Appl Surf Sci 2017;421 508–512.
[9] Zhang XN, Qiu J, Li XC, Zhao JM, Liu LH. Complex refractive indices measurements of polymers in visible and near-infrared bands. Appl Opt 2020;59(8) 2337–2344.
[10] Wang CC, Tan JY, Ma YQ, Liu LH. Infrared optical constants of liquid palm oil and palm oil biodiesel determined by the combined ellipsometry-transmission method. Appl Opt 2017;56(18) 5156–5163.
[11] Wang CC, Tan JY, Liu LH. Wavelength and concentration-dependent optical constants of NaCl, KCl, $MgCl_2$, $CaCl_2$, and Na_2SO_4 multi-component mixed-salt solutions. Appl Opt 2017;56(27) 7662–7671.
[12] Woollam Co JA. Guide to using WVASE32: spectroscopic ellipsometry data acquisition and analysis software. JA Woollam Company; 2008.
[13] Collins RW, An I, Fujiwara H, Lee J, Lu Y, Koh J, et al. Advances in multichannel spectroscopic ellipsometry. Thin Solid Films 1998;313:18–32.
[14] Zhang ZM. Nano/microscale heat transfer. McGraw-Hill; 2007.
[15] Zhang ZM, Lefever-Button G, Powell FR. Infrared refractive index and extinction coefficient of polyimide films. Int J Thermophys 1998;19 905–916.
[16] Xie BW, Ma LX, Zhao JM, Liu LH, Wang XZ, He YR. Experimental study of the radiative properties of hedgehog-like ZnO–Au composite particles. J Quant Spectrosc Radiat Transf 2019;232:93–103.
[17] Hughes IG, Hase TPA. Measurements and their uncertainties: a practical guide to modern error analysis. Oxford; 2010.
[18] Schneider F, Draheim J, Kamberger R, Wallrabe U. Process and material properties of polydimethylsiloxane (PDMS) for Optical MEMS. Sens Actuators A 2009;151(2):95–9.
[19] Querry MR. Optical constants of minerals and other materials from the millimeter to the ultraviolet, chemical research, development & engineering center. US Army Armament Munitions Chemical Command; 1987.
[20] Cai D, Neyer A, Kuckuk R, Michael HH. Raman, mid-infrared, near-infrared and ultraviolet–visible spectroscopy of PDMS silicone rubber for characterization of polymer optical waveguide materials. J Mol Struct 2010;976(1–3) 274–281.
[21] Beadie G, Brindza M, Flynn RA, Rosenberg A, Shirk JA. Refractive index measurements of poly (methyl methacrylate) (PMMA) from 0.4-1.6 μm. Appl Opt 2015;54(31) 139–143.
[22] Cariou JM, Dugas J, Martin L, Michel P. Refractive-index variations with temperature of PMMA and polycarbonate. Appl Opt 1986;25(3) 334–336.
[23] Lucarini V, Saarinen JJ, Peiponen K-E, Vartiainen EM. Kramers-Kronig relations in optical materials research. Springer; 2005.
[24] Sultanova N, Kasarova S, Nikolov I. Dispersion properties of optical polymers. Acta Phys Pol 2009;116(4) 585–587.
[25] Zimmerer C, Ziegler L, Heinrich G, Steiner G. Time resolved characterization of the solid-state reaction between polycarbonate and primary amine. Eur Polym J 2018;98 313–320.
[26] Jitian S. Determination of optical constants of polystyrene films from ir reflection-absorption spectra. Analele Universităţii “Eftimie Murgu” Reşiţa 2011;48:41–8.
[27] Biron M. Thermoplastics and thermoplastic composites. 2nd Edition. William Andrew; 2013.
[28] Hinrichs K, Eichhorn KJ. Combined infrared and visible spectroscopic ellipsometry study of thin polymer layers. Spectrosc Eur 2007;19(6):11–14.
[29] Midgley JT, Henne AL, Leicester HM. Natural and synthetic rubber. XVI. The structure of polystyrene. J Am Chem Soc 1936;58(10) 1961–1963.
[30] Dybal J, Schmidt P, Baldrian J, Kratochvil J. Ordered structures in polycarbonate studied by infrared and Raman spectroscopy, wide-angle X-ray scattering, and differential scanning calorimetry. Macromolecules 1998;31(19) 6611–6619.
[31] Bower DI, Jackson RS. Vibrational assignments for the CCL stretching region of the Raman spectrum of poly (vinyl chloride). J Polym Sci, Part B 1990;28(9) 1589–1598.
[32] Mutel B, Dessaux O, Goudmand P, Gengernbre L. Energy consumption and kinetic evolution of nitrogen fixation on polyethlene terephthalate by remote nitrogen plasma: XPS study. Surf Interface Anal 1993;20(4) 283–289.
[33] Seifert B, Mihanetzis G, Groth T, Albrecht W, Richau K, Missirlis Y, et al. Polyetherimide: a new membrane-forming polymer for biomedical applications. Artif Organs 2015;26(2) 189–199.
[34] Chawla M, Rubi R, Kumar R, Sharma A, Aggarwal S, Kumar P, et al. Tailoring structural properties of polyethylene terephthalate (PET) by 200 keV Ar^+ implantation. Adv Mater Res 2013;665 221–226.
[35] Vora RH, Goh SH, Chung TS. Synthesis and properties of fluoro-polyetherimides. Polym Eng Sci 2000;40(6) 1318–1329.
[36] Porter SG. A brief guide to pyroelectric detectors. Ferroelectrics 1981;33(1):193–206.